BHPA-symposium 2022

Scientific Committee

Milan Tomsej (chair), CHU Charleroi

Alain Seret, Université de Liège

Caro Franck, Universitair Ziekenhuis Antwerpen

Damien Dumont, UCLouvain

Kristof Baete, KU Leuven

Lara Struelens, SCK-CEN

Federica Zanca, Palindromo

Koen Tournel, Jessa Ziekenhuis

Nico Buls, UZ Brussel

Gert Van Gompel, UZ Brussel

Thierry Gevaert, UZ Brussel

Poster Session

Foyer Auditorium 2000

Can radiomics of cardiac magnetic resonance parametric mapping contribute to the diagnosis?

T. Dresselaers[1], P. Rafouli-Stergiou[1], R. De Bosscher[2], S. Tilborghs[3], C. Dausin[4], A. Cernicanu[5], P. Claus[2], R. Willems[2], G. Claessen[2], J. Bogaert[1]

[1]KU Leuven, Dept of Imaging and Pathology, Leuven, BE, [2]KU Leuven, Dept of Cardiovascular Sciences, Leuven, BE, [3]KU Leuven, Dept. of Electrical Engineering (ESAT), Leuven, BE, [4]KU Leuven, Exercise Physiology Research Group, Leuven, BE [5]Philips BE, Eindhoven, The Netherlands.

ABSTRACT - It was our hypothesis that a radiomics analysis of cardiac MRI parametric mapping images would identify features that can benefit the diagnosis of certain myocardial diseases. We determined the feasibility by evaluating the potential of radiomics to discriminate an athlete's heart from hypertrophic cardiomyopathy. We observed that classification based on only two radiomics features outperformed the conventional approach based on average T1 values.

KEY WORDS – MRI, Heart, Radiomics, T1 mapping, Hypertrophy

Introduction

In cardiac magnetic resonance (CMR) imaging, parametric T1 and T2 mapping has caused a paradigm shift in the study of myocardial diseases. These T1 and T2 maps provide quantitative values that allow a more objective comparisons between subjects and across diseases. In addition, by combining pre - and post contrast T1 maps an extra-cellular volume (ECV) map, indicative of fibrosis, can be derived. Analysis of CMR mapping data is however time consuming and hence often restricted to an average regional myocardial value. An automated radiomics analysis can derive more "features" describing the complex image texture present. Such radiomics methods have recently shown improved diagnostic accuracy over conventional qualitative methods. Only few studies have however applied radiomics to CMR mapping data [1-3]. Here we aimed to demonstrate that a radiomics approach provides superior capacity to distinguish hyperthropic cardiomyopathy (HCM) from athlete's heart over average T1 and ECV values. Differentiating intensive training induced hypertrophy from HCM is important to identify athletes at risk of sudden cardiac death.

Materials and methods

This study included data from 97 subjects diagnosed with HCM (acc. to guidelines; [4]) and 28 athletes that took part in the Master@Heart trial [5]. T1 mapping data was acquired on a 1.5T Philips Ingenia system using MOLLI [6]. After respiratory motion correction and T1 and ECV map calculation [7], the left ventricular myocardium was manually delineated (3D Slicer; [8]). The radiomics analysis resulted in 194 features (Pyradiomics, [9]). The dataset was then split (75/25%) for training and testing purposes. A fast correlation based filter rank was applied to the training data to derive relevant features. A further reduction to only two

features was based on the CA of a support vector machine (SVM) learning method. Finally, the diagnostic accuracy (ROC analysis; [10]) in the test data for the following predictors was determined: 1) median T1 and ECV 2) two most relevant features (training) 3) (1) and (2) combined.

Results

The two most relevant features were the histogram feature 'ECV energy' and the gray level size zone matrix (GLSZM) 'native T1 zone entropy' feature, a measure of heterogeneity in the texture pattern. A model to distinguish HCM from athletes based on these features outperformed the model using only median T1 and ECV values with both higher sensitivity and specificity (table 1) and a significantly higher AUC in the ROC analysis ($p<0.05$, figure 1). Combining these two features with median values did not improve the CA further.

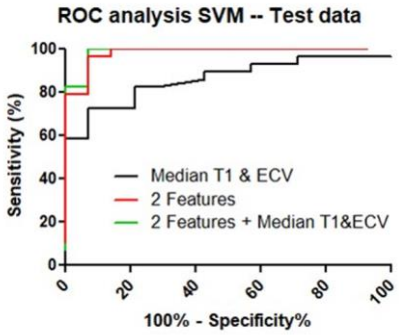

Figure 1: ROC analysis of three predictor models to discriminate subjects with a remodeled heart due to intensive training from subjects suffering from HCM. The two most relevant features based on the training set outperformed classification based on the conventionally used average T1 and ECV values.

Test dataset				
	AUC	CA	Precision	Specificity
2 sel. feat. (ECV energy, native T1 zone entropy)	0.983	0.907	0.914	0.918
2 sel feat. & Median T1 & ECV	0.988	0.907	0.914	0.918
Median T1 & ECV	0.862	0.814	0.823	0.799

Table 1: AUC, classification accuracy (CA), precision and specificity test dataset result according to the different predictor models. The two features derived from the training dataset also showed improved CA on the test data.

Conclusion

Radiomics of T1 and ECV mapping out-performed classical analysis in distinguishing HCM from athlete's heart. The robustness and broader applicability of CMR radiomics features need to be further evaluated.

References

[1] Neisius et al. JACC: cardiovasc. Imag. 2019; 12(10): 1946-54; [2] Shi RY et al. Clin Radiol. 2021;76(3):236.e9-236.e19. [3] Baessler B et al. Radiology. 2019;292(3):608-617. [4] Gersh et al. J Am Coll Cardiol 2011;58:e212–60. [5] De Bosscher et al. BMJ Open Sport Exerc Med. 2021 Apr 16;7(2):e001048 [6] Kellman P, Hansen MS. J Cardiovasc Magn Reson. 2014;16:2 [7] Tilborghs S et al. MedIA, 2019: 212-227 [8] Fedorov A. et al. Magn. Reson. Imag.. 2012;30(9):1323-41. [9] van Griethuysen et al. Cancer Res., 2017; 77(21), e104–e107. [10] Sun X and Xu W, IEEE Signal Proc. Letters 2014; 21 11): 1389-1393.

Skin dosimetry model for CT acquisitions

Mahta Mazloumi[1], Margo Cabuy[1], Gert Van Gompel[1], Johan de Mey[1], Nico Buls[1]

[1] Vrije Universiteit Brussel (VUB), Universitair Ziekenhuis Brussel (UZ Brussel), Department of Radiology, Laarbeeklaan 101, 1090 Brussels, Belgium

KEY WORDS

Computed Tomography, Skin dose, Monte Carlo simulations, Skin dose model, acquisition parameters

Introduction

Skin is the first organ that is exposed to X-ray during a CT scan and it can receive a relatively high radiation dose in CT procedures with repeated exposure of the same skin area such as interventional or perfusion CT. The aim of this study is to provide a skin dose model based on CT acquisition parameters to allow dose follow up for this organ at risk.

Materials and methods

A virtual cylindrical phantom was generated (32 cm, L=20 cm, pixel size=0.5 mm^2) in DICOM format. The phantom was used as a 3D geometrical model for Monte Carlo (MC) simulations with ImpactMC (Advanced Breast-CT). The impact of acquisition parameters including tube voltage (70, 80, 100, 120, and 140 kVp), bow-tie filter (medium, large), and position in the gantry on skin dose were investigated with the MC simulations. The boundary pixels at the outer layer of the phantom were considered as the skin (thickness 0.5 mm^2). The dose values were normalized to $CTDI_{vol}$ (D_{CTDI}). In addition, the model was validated with experimental TLD measurements and MC simulations on humanoid Rando Alderson (RA) phantom for large filter at 120 kVp and 80-mm collimation.

Results

The results show an increase in the skin dose with decrease in the distance to the isocenter (Figure 1). For distances smaller than 120 mm four curves were fitted to the data for high voltage (100, 120, 140 kVp)-medium bow-tie filter, low voltage (70, 80 kVp)-medium bow-tie filter, high voltage-large bow-tie filter, and low voltage-large bow-tie filter. For distances larger than 120 mm, we fitted a single curve for all the tube voltages and filter types (Figure 1, Table 1). In addition, the skin dose values of RA phantom were in a good agreement with our model at 120 kVp and large filter (Figure 2). The average deviation between the experimental TLD measurement on RA phantom and the MC simulations of RA phantom were 9%.

Conclusion

Our skin dose model can be used to estimate the skin dose as a function of filter type, tube voltage, and distance to the iso-center. This allows the automatization of skin dosimetry based on CT images and scan parameters. In addition, this model allows estimating the skin dose prior to the CT scan, based on the selected parameters and the scout views.

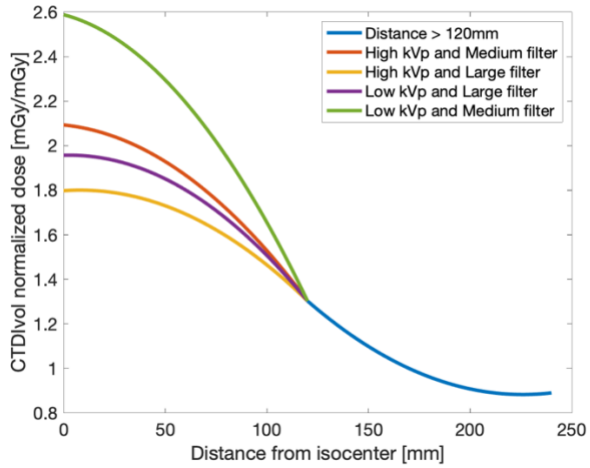

Figure 1: General skin dose model as a function of filter type, tube voltage and distance to the iso-center.

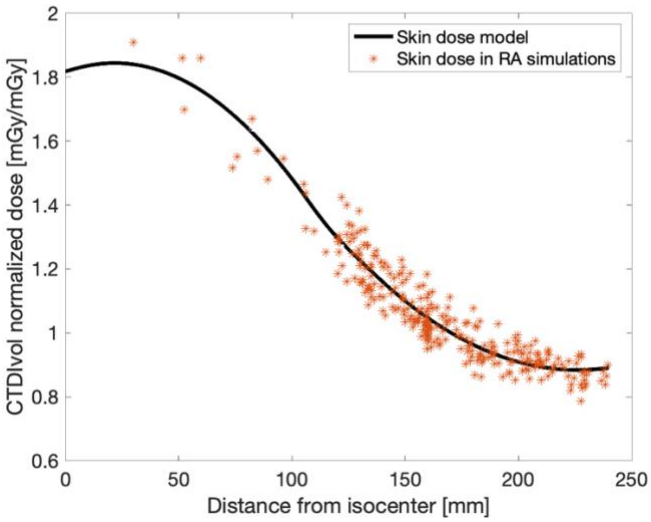

Figure 2: D_{CTDI} as a function of distance to iso-center based on the skin dose model and RA simulations.

Distance to the isocenter (mm)	**Tube voltage (kVp)**	**filter**	**D_{CTDI} =A*x(mm)² + B*x(mm)+C**
Larger than 120	70, 80, 100, 120, 140	Medium filter, large filter	A = 3.74E-05, B = -0.02, C= 2.79
Smaller than 120	100, 120, 140	Medium filter	A = -4.71E-05, B= -92.95E-05, C= 2.09
Smaller than 120	100, 120, 140	Large filter	A=-3.96E-05, B= 62.58E-05, C= 1.80
Smaller than 120	70, 80	large filter	A=-4.75E-05, B= 25.49E-05, C= 1.96
Smaller than 120	70, 80	Medium filter	A=6.92E-05, B= -240E-05, C= 2.59

Table 1: General skin dose model based on filter type, tube voltage and distance to the iso-center.

Evaluation of scatter correction methods in ^{166}Ho SPECT by Monte-Carlo simulations and phantom measurements, including the impact on personalized dosimetry in SIRT

Marie Mannie-Corbisier[1], Benoît Collette[2], Nicola Trotta[2], Nicolas Pauly[1], Ana-Maria Bucalau[3], Gontran Verset[3], Serge Goldman[2] and Rodrigo Moreno-Reyes[2]

From the [1]Department of Nuclear Metrology, Ecole polytechnique de Bruxelles, Université libre de Bruxelles (ULB), Brussels, Belgium.

From the [2]Department of Nuclear Medicine, Hôpital Erasme, Université libre de Bruxelles (ULB), Brussels, Belgium.

From the [3]Department of Gastro-Enterolgy, Hôpital Erasme, Université libre de Bruxelles (ULB), Brussels, Belgium.

ABSTRACT : The complexity of the scatter components in ^{166}Ho SPECT leads to various questions in terms of image quality optimization, quantification, and dosimetry. The aims of this work are to study scatter correction methods to propose a suitable and portable method on available SPECT systems, and to estimate the impact of this choice on image quality and dosimetry using imaging and Monte-Carlo simulations. **KEY WORDS :** Holmium-166, SIRT, TARE, personalized dosimetry, Monte-Carlo simulation.

Introduction

Developments in transarterial radioembolization (TARE) in the treatment of liver cancers, a particular case of selective internal radiotherapy (SIRT), implied the creation, the use, and the study of new microspheres loaded with ^{166}Ho. However, due to the complexity of the scatter components in ^{166}Ho SPECT, various questions in terms of image quality optimization, quantification, and dosimetry are emerging. The aims of this work are to study scatter correction methods to propose a suitable and portable method on available SPECT systems, and to estimate the impact of this choice on image quality and dosimetry using imaging and Monte-Carlo simulations.

Materials and methods

A dual energy window method and a triple energy window method were chosen and compared. This study was realized on a hybrid SPECT/CT system, the Philips BrightView XCT, with Medium Energy collimators. First, Monte-Carlo simulations of simple sources geometries acquisitions were carried out with GATE 7.0 software (based on Geant4) to assess the different scatter components in the different energy windows used. It also allowed to confirm the choice of the parameter k needed for the dual energy window method. Then, Monte-Carlo simulations of acquisitions of a Jaszczak SPECT phantom filled with a ^{166}HoCl solution were made with specific conditions mimicking an ideal scatter correction. These simulated projections can be reconstructed and compared with real acquisitions corrected by both methods and reconstructed in the same way. Finally, both methods were applied on patient data (from TARE simulations and post-treatment imaging), and the impact on dosimetry was evaluated.

Results

Monte-Carlo simulations confirmed the use of k = 1 for dual energy window method in the context of ^{166}Ho imaging. Regarding spectroscopy, these simulations also confirmed the complexity of scatter components in the main energy window used with a high energy gamma rays component around 50 % of the total counts detected, but a negligible X rays component and a negligible influence of fluorescence (*Figure 1*). Simulated projections of simple geometries suggested a loss of spatial information using the dual energy window method. Contrast recovery coefficients analysis, made on simulated scatter-free projections of the phantom and on scatter corrected acquisitions of the same phantom, suggested a better efficiency of the triple energy window method (*Figure 2*). Finally, these methods were applied on patient data showing significant differences in terms of non-tumoral liver absorbed dose, non-tumoral liver fraction under 50 Gy, and tumor absorbed dose (*Figure 3*).

Conclusion

This study demonstrated the impact of scatter correction on personalized dosimetry. The use of a triple energy window method is proposed for scatter correction in ^{166}Ho SPECT.

Figure 1 : Simulated spectrum including the energy windows used

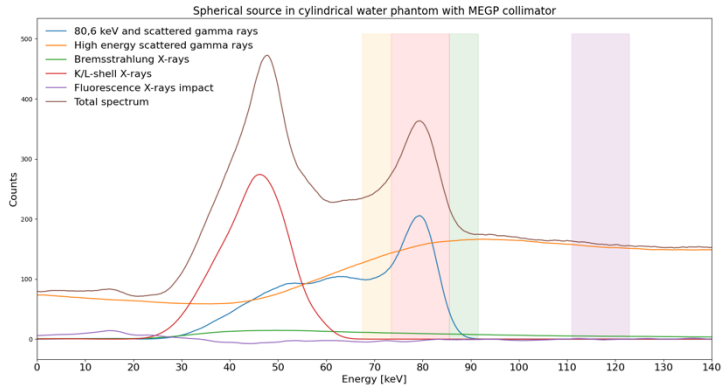

Figure 2 : Contrast recovery coefficients

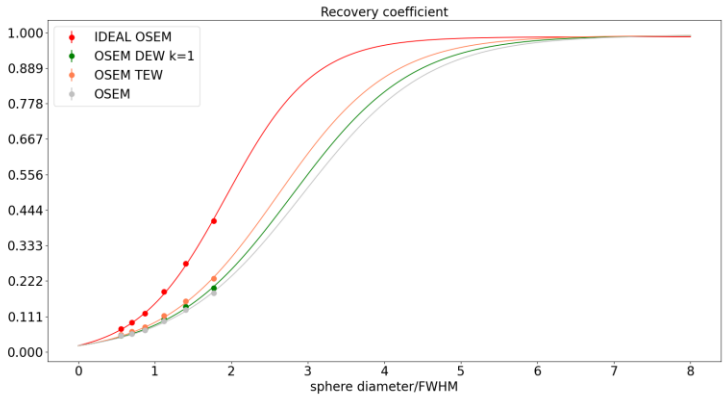

Figure 3 : Example comparing DEW and TEW method applied on patient data including the impact on dosimetry

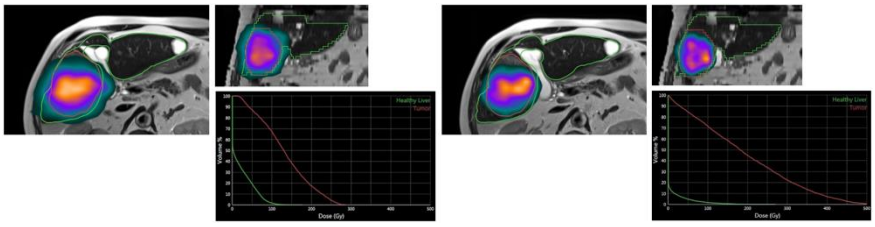

Off Axis Linac QA for SIMT using a Ruby insert prototype (PTW)

A. Monseux[1], V. Baltieri[1], J-L. Greffe[1], C. Leclercq[1], A.Sottiaux[1], D. Vanache[1], M.Tomsej[1]
[1]CHU Charleroi, Belgium

ABSTRACT

Winston **L**utz and **H**idden **T**arget **T**ests are well known and useful checks to evaluate the linac and repositioning system precision and robustness for stereotactic treatments. **S**ingle **I**socentre for **M**ultiple **T**argets is more and more adopted in radiotherapy departments to treat several metastases, but consequently, these are no longer in the isocentre plane.

The objective of this work is to study the linac and repositioning system precision with a Ruby insert prototype from PTW when moving away from the isocentre.

KEY WORDS

Hidden target test, Winston-Lutz test, linac off axis precision, SIMT, Ruby insert prototype

Introduction

Single Isocentre for Multiple Targets technique is more and more adopted in radiotherapy department to treat several metastases in one session. But then, they are no longer in the isocentre plane. Consequently, the traditional Winston Lutz and Hidden target tests QA with only one ball located in the isocentre could be not enough to assess the linac precision and the capacities of the repositioning system in plans away from the isocentre.

Materials and methods

First, a CT scan of the Ruby phantom is carried out using the insert prototype containing 5 ceramic balls at different positions in the 3 directions. A plan with MLC apertures centered on the balls was created for several gantry angles (0°, 90°,180° ,270°) and 2 collimator rotations (0° and 90°). The isocentre is set on the central ball. In a second time, we positioned the phantom with the lasers or with the Exactrac system and acquired portal imaging of the different fields.

Finally, for each image, a measurement of the distance between the MLC aperture centre and the ball centre (Δx and Δy) is performed and the size of the ellipsoid, the error of positioning and the total offset =

V((Δx)²+(Δy)²) is evaluated. For the balls not located in the isocentre plane, their positions are corrected for the beam divergence.

Results

Positioning errors have been found to be less than 1mm in most of the cases when introducing translation errors only. Probably due to the lack of structures for the matching, Exactrac system is less precise when rotational errors are introduced.

The diameter of the ellipsoid described by the linac is function of the ball position and is smaller than 1.5 mm for all investigated distances.

The total offset does not seem to be correlated with the ball position and is less than 1mm in average.

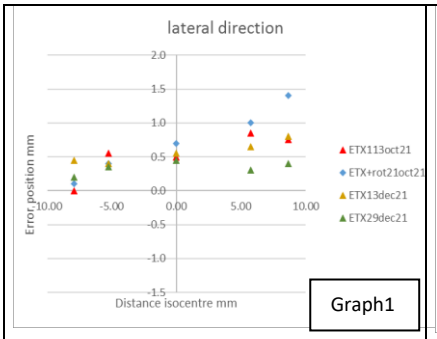

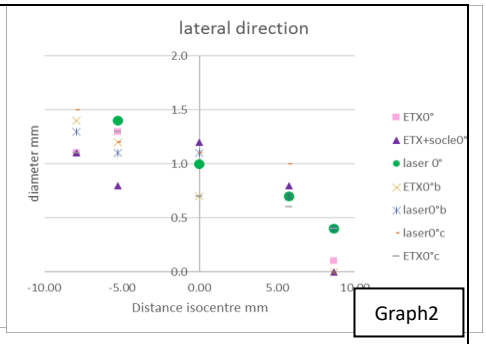

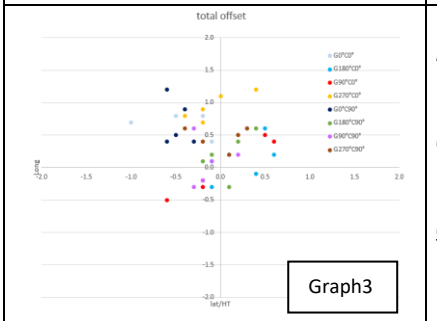

Graph1 : Positioning error with ETX in lateral direction.

Graph2 : Ellipsoid diameter in lateral direction.

Graph3 : Total offset for different gantry and collimator position.

Conclusion

The first results are confident and can help in the decision of strategy margin. The procedure is useful to evaluate the ETX calibration but the quality of the test should be improved with the addition of structures regarding matching. Lack of software makes the analyses time consuming and probably less precise.

References

[1] Gao J., Liu X. Winston-Lutz-Gao Test on the Truebeam Stx linear accelarator. International journal of medical physics, clinical engineering and radiation oncology, 2019, 8,9-20.
[2] PTW, Ruby Manual T40072, 2021

Characterization of a novel algorithm for fast iterative PET reconstruction

Nuttens Victor
KU Leuven

ABSTRACT

KEY WORDS – PET, SPDHG, Reconstruction algorithm, Subsets

Introduction

The goal is to evaluate a newly proposed PET reconstruction algorithm called SPDHG (Stochastic Primal Dual Hybrid Gradient algorithm) which is supposed to outperform OSEM.

Materials and methods

The performance is evaluated on the basis of a relative cost function (the relative log-likelihood), of the PSNR (Peak Signal-to-Noise Ratio, with reference MLEM) of the post-smoothed images, of the bias and uncertainty of the mean recovery values in different ROIs. 2D-realistic virtual phantoms were used.

Results

The relative cost is lower for SPDHG and that after typically 20 iterations. The PSNR of the post-smoothed images is higher for SPDHG when compared to OSEM. The mean recovery and bias versus RSD (Relative Standard Deviation) plots show that in all cases the RSD is lower for SPDHG than for OSEM. The reconstructions showed that in certain cases the limit cycle of OSEM does not show small objects in noisy environments (see figure 1), while the detectability of SPDHG resembled that of MLEM.

Conclusion

For the right step size ratio, SPDHG converges to the maximum-likelihood solution and has the potential to be even faster than OSEM since fewer projections per subset can be used. SPDHG also has lower uncertainty which gives SPDHG better test-retest reliability.

Figure 1: Detectability of the smallest sphere in SPDHG versus OSEM for different noise realisations

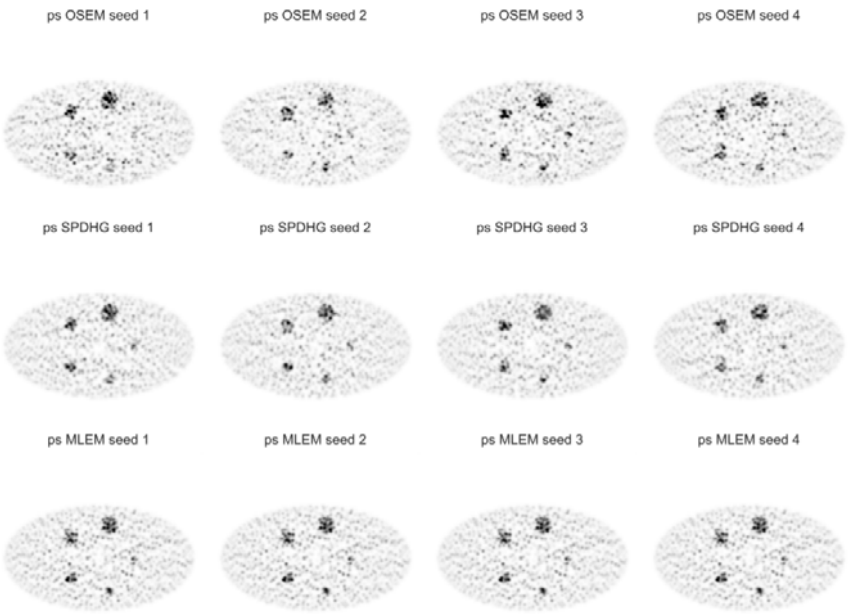

References

[1] M. J. Ehrhardt, P. Markiewicz, and C.-B. Schönlieb, “Faster PET reconstruction with non-smooth priors by randomization and preconditioning,” Physics in Medicine & Biology, vol. 64, no. 22, p. 225019, nov 2019. [Online]. Available: https://doi.org/10.1088%2F1361-6560%2Fab3d07

Keynote information of the NCS report 34 : Code of Practice and recommendations for Total Body Irradiation and Total Skin Irradiation

Geert Pittomvils [1]
[1]*UZ Gent, C. Heymanslaan 10, 9000 Gent*

ABSTRACT – The aims of this report are multiple : to provide a guideline for institutes that are considering starting up TBI/TSI treatments; standardization of the actual manual workflow; creation of a reference in order to benchmark the individual institution protocol allowing guided improvement and description of novel techniques already developed in center of excellence in order to guide and accelerate the evolution towards new treatment techniques.

KEY WORDS – Total Body Irradiation, Total Skin Irradiation, Quality Assurance, Risk Analysis

Introduction

While Total Body Irradiation (TBI) and Total Skin Irradiation (TSI) differ significantly to standard irradiation techniques, a special dedicated quality assurance process is recommended. Therefore a survey was sent around to investigate the actual status of the treatment protocols and quality assurance confirming our expectation : despite many decades of experience and previous surveys, a large variety remained in treatment protocols, being a combination of evolved traditional and more modern CT-base irradiation techniques.

Materials and methods

The survey revealed three different workflows for TBI: a manual workflow (11); a TPS workflow (5) and a sweeping technique workflow (1). The report is focusing on the main topics of the treatment process : commissioning guidelines, pre-treatment and treatment delivery guidelines and a risk analysis. Unlike TBI, the guidelines for the TSI can be limited to guidelines for a manual workflow.

Results

Recommendations for the commissioning process are made for absolute dose calibration, beam flatness, PDD's, in vivo dosimetry systems, dry runs/end-to-end tests and in vivo dosimetry. Extra positioning devices for both TBI and TSI treatment techniques are also included. Dedicated for TBI are shielding recommendations, commissioning steps for the TPS

workflow and guidelines for the extra measurements for sweeping techniques. Infrastructure issues for both techniques are also included.

Pretreatment workflow topics are discussed for the manual TBI/TSI and TPS TBI workflow in combination with recommendations for single and multiple fraction treatment delivery including in-vivo tolerances for both TBI and TSI treatments.

Risk analysis is performed for both the process of developing and introducing a TBI/TSI technique and failures in the process branch of the TBI/TSI clinical workflow and scored for severity and frequency. 47 processes are scored in this risk analysis; helping the reader to optimize their own treatment process.

Conclusion

This report is a step in the process in the evolution to a state-of-the-art treatment technique. This does not develop any new techniques. Instead, it describes current practiced techniques and possible guidelines to implement such techniques clinically. This report provides a stepping stone for achieving more high-quality treatment processes.

References

[1] Murrer L., Van der Hulst P, Janssens W., van Leeuwen R. et al. Code of Practice and recommendations for Total Body Irradiation and Total Skin irradiation. *NCS Dosimetry Report nr. 34.* 2021. doi.org/10.25030/NCS-034

Portal imaging used as a dosimetry QA tool for SRS treatments planned with non Varian TPS

M.Tomsej[1], V.Baltieri[1], J. Fagnart[2], C. Leclercq[1], A. Monseux[1], A. Sottiaux[1], D. Vanache[1]

[1]CHU de Charleroi, Department of Radiation Medical Physics, Charleroi, Belgium

[2]Université de Namur, Namur, Belgium

ABSTRACT – SRS treatments requests very precise patient dedicated dosimetry QA. However, classical (point dose detector and film) QA is extremely time consuming, and could be substituted by portal imaging devices. This does represent a challenge as planning is performed with a non Varian Planning System. This study allowed to determine optimal parameters in order to use safely portal dosimetry.

KEY WORDS – Quality assurance, portal imaging, SRS.

Introduction

In the framework of QA for SRS treatments, classical means are extremely time consuming, using point dose detectors and radiochromic films. In order to reduce the workload for this patient dedicated dosimetry check, portal imaging devices could be used as for IMRT/VMAT treatments. Obviously, this solution has to be completely safe and reliable by selecting optimal parameters.

Materials and methods

Methodology consists in comparing predicted dose calculated by PDIP algorithm and measurements performed by portal imaging device delivering the treatment plan of the patient. The analysis is carried out using gamma calculation method using optimal DTA and dose parameters in order to make QA as much sensitive as possible to detect errors.

Results

First results are obtained using standard parameters for the gamma analysis. They indicate to be reduced to get patient dedicated QA more sensitive. DTA, dose and comparison region size have been much lowered (final parameters: 3%, 1.5 mm, MLC + 2 mm), as negative results are found for 15 % of cases.

Figure1:

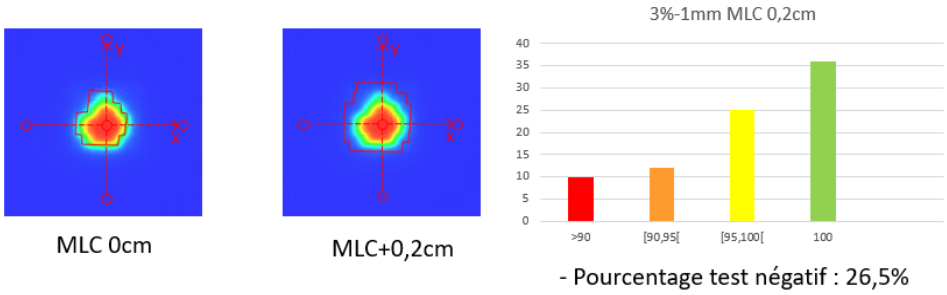

Conclusion

Finally, this study has shown that recommended gamma analysis parameters are DTA: 1.5 mm, dose: 3%, region of comparison: MLC + 2 mm if one chooses to use portal imaging as a dosimetry QA tool for clinical treatment plans calculated with a non-VARIAN TPS (iPlan/Elements, Brainlab). Then, a tentative of determination of origins of negative tests has been carried out.

References

[1] T. A. Hadi. La mesure et la modélisation des faisceaux de photons de petite taille pour l'IMRT et la radiochirurgie. Traitement du signal et de l'image [eess.SP]. Université Paul Sabatier - Toulouse III, 2017. Français. ffNNT : 2017TOU30056ff. fftel-01825782f.

[2] D.A. Low, W.B. Harms, S. Mutic, J.A Purdy. A technique for the quantitative evaluation of dose distributions. Med Phys. 1998 ;25 :656□661. - PubMed.

[3] M. Hussein, P. Rowshanfarzad, M.A. Ebert, A. Nisbet, C.H. Clark. A comparison of the gamma index analysis in various commercial IMRT/VMAT QA systems. Radiotherapy and Oncology 2013 ;109 :370-376.

[4] A. R. Barbeiroa, L. Parent, L. Vieillevignea, R. Ferranda, X. Franceriesa. Dosimetric performance of continuous EPID imaging in stereotactic treatment conditions. Med Phys. 2020 ;78 :117-122.

[5] L.Berger. Utilisation d'un système d'imagerie portale électronique avec détecteur au silicium amorphe pour vérifier la dose reçue par les patients en radiothérapie. Université Paul Sabatier - Toulouse III, 2006

What the interventional radiologist expects from the clinical physicist

It is essential to have good medical physicists in a radiology department. With the increasing awareness about radiation protection in the last decade, major steps have been made in reducing dose in conventional X-ray imaging, CT scanning and in the angiography suite. Often a special division in the radiology department, interventional radiologists are a major service provider for referring physicians. Working long procedures, often at irregular times, standing next to the patient, it is of utmost importance to have good radiation protection and a well-organized angiography suite. This benefits the patient, the treating interventionalist and the staff that is present in the room. How this is done, will be briefly explained is this abstract.

Everything starts with involving the medical physicist from the beginning. Acquiring a new angiography suite, although a major investment, can significantly reduce dose with the improved technology. This is a first step in which the medical physicist can assist in making the right choice. Others important factors involved include the user interface, ergonomic aspects, ease of use and maintenance, aftersales service level and so on.

Installing the angiography suite requires good planning. Well thought of position of the lead screens, allowing easy manipulation, being it moving in or moving out, will lead to an increased and oftentimes better use.

With the vendor installing the different programs on the machine, there is another important moment for the clinical physicist to evaluate the settings to make sure no faulty features have slipped in.

Consent with local regulations must be verified. Since about a year, as defined by a royal decree on medical exposure, we now must implement two optimalisations every year. Additional major steps in reducing radiation will not be easily achieved, but we will need to be thinking what can be done. Examples given: defining high risk zones for staff present in the angiography suite, providing yearly reports on radiation dose for different procedures, finding ways to reduce dose even further without losing imaging quality.

To achieve optimal results, close collaboration at all phases is necessary. This can be most easily implemented by having a permanent hospital physicist. Good communication will benefit both parties as we both (medical physicists and interventional radiologists) have our blind spots for things that might be evident for the other party.

References:

1. Essential Role of a Medical Physicist in the Radiology Department. Mahadevappa Mahesh Radiographics Oct 10 2018 https://doi.org/10.1148/rg.2018180111
2. RAF/6/038 Promoting Regional and National Quality Assurance Programmes for Medical Physics in Nuclear Medicine CLINICAL TRAINING PROGRAMMES AND PORTFOLIOS FOR THE REGIONAL TRAINING IN NUCLEAR MEDICINE AND DIAGNOSTIC/INTERVENTIONAL RADIOLOGY MEDICAL

PHYSICS REPORT OF A TASK FORCE MEETING 2014 Recommendations for Medical Physics Education in AFRA Member States
https://humanhealth.iaea.org/HHW/MedicalPhysics/TheMedicalPhysicist/EducationandTrainingRequirements/Educationalrequirements/AFRA_Clinical_training_-_Imaging_medical_physics.pdf